First-principles study of stability and local order in substitutional Ta-W alloys

P. E. A. Turchi and A. Gonis
Lawrence Livermore National Laboratory, L-353, P.O. Box 808, Livermore, California 94551

V. Drchal and J. Kudrnovský
Institute of Physics, Academy of Sciences of the Czech Republic, Na Slovance 2, CZ-180 40 Praha 8, Czech Republic
(Received 19 January 2001; published 8 August 2001)

A parameter-free electronic structure approach is applied to the study of stability and chemical order in substitutional bcc-based Ta-W alloys. The method is based on a Green's function description of the electronic structure of the random alloys. Configurational order is treated within the generalized perturbation method, and temperature effects are examined with a generalized mean-field approach. In contrast to the results summarized in the assessed phase diagram, an unambiguous tendency toward order with a $B2$ superstructure in a broad range of alloy composition is predicted. The details of the thermodynamics analysis, phase diagram, and short-range order are given for Ta-W alloys as a function of temperature and concentration.

DOI: 10.1103/PhysRevB.64.085112 PACS number(s): 71.20.Be, 61.66.Dk, 64.60.Cn

I. INTRODUCTION

Much attention has been paid to alloys made of refractory metals of columns VB and VIB of the Periodic Table, and in particular, Nb, Mo, Ta, and W that display high melting points. These alloys show excellent strength at elevated temperature and therefore have been found useful for high-temperature space and nuclear applications. As part of a more extended and systematic study of this class of alloys, in the present paper we focus on Ta-W alloys.

According to the assessed phase diagram, Ta-W substitutional alloys should display complete solubility in the solid phase with a body-centered cubic (bcc, or α) crystalline structure up to the solidus-liquidus line.[1] Although no intermediate phases have been reported in the literature, there are indications that chemical order may exist in this alloy system. Indeed it has been shown experimentally that the variation of the lattice parameter with composition displays a negative departure from Vegard's law,[2] and also that the activities of both elements determined at 1200 K indicate negative deviation from Raoult's law and therefore ideality.[3] Furthermore, the measured negative excess free energies of mixing are attributed to mostly negative enthalpies of mixing and also small negative excess entropies of solution.[2,3] These sparse experimental facts have led us to reexamine this alloy system with a first-principles approach to stability and chemical order. Our focus will be primarily on the short-range order (SRO) taking place at high temperature in the α solid solution. The configurational order will be examined within the generalized perturbation method (GPM).[4,5] The electronic structure properties of the reference medium on which the GPM relies are described in the framework of the self-consistent tight-binding linear muffin-tin orbital (TB-LMTO) multiple-scattering formulation of the coherent potential approximation (CPA).[5,6] Finally, temperature effects on local order and stability will be examined by means of a standard generalized mean-field approach, namely, the cluster-variation method (CVM).[7]

From our thermodynamic analysis, Ta-W alloys should exhibit a definite tendency toward order with a $B2$ superstructure of CsCl type. Our analysis also reveals a low-lying phase diagram that supports the experimental findings discussed above. These results will be simply explained in terms of the average number of valence electrons and the difference in the number of valence electrons of the alloy constituents.

The paper is organized as follows. In Sec. II, we discuss the electronic structure properties of Ta-W alloys based on the first-principles TB-LMTO-CPA results. In Sec. III, tendencies toward order or phase separation are examined in the context of the GPM. It will be shown that the nature and the strength of local order in this alloy can be well explained in terms of simple electronic parameters. In Sec. IV, the influence of temperature on stability and local order is studied with a standard generalized mean-field approach. The coherent phase diagram for bcc-based Ta-W is predicted, and the SRO results are discussed before the results are summarized in Sec. V.

II. ELECTRONIC STRUCTURE PROPERTIES

As far as we know, electronic structure studies of Ta-W alloys based on a proper treatment of the disordered alloys have not been reported till date. The motivation for the use of a quantum-mechanical-based methodology is the desire to perform an unbiased study of Ta-W alloys, in which the resulting thermodynamic behavior is determined on the basis of *ab initio* obtained interaction parameters that are free of imposed constraints, parametrization schemes, or fitting procedures. The single-site CPA, expressed with the Green's function formalism and implemented within the TB-LMTO-CPA, provides an appropriate basis for such a study.[8]

This methodology allows the determination of an effective medium whose scattering properties on the average reflect those of a chemically random alloy. Calculations based on this method yield such relevant physical properties as equilibrium lattice constants, energies of mixing, and bulk moduli for substitutionally disordered alloys. The effects of statistical fluctuations away from this average medium can be studied through GPM (Refs. 4 and 5) which leads to

uniquely defined, concentration-dependent effective cluster interactions (ECI). When used in conjunction with a statistical model, such as CVM,[7] these concentration-dependent effective interactions lead to the prediction of the most stable ordered structures at zero temperature, and of concentration/temperature alloy phase diagrams.[9]

For bcc-based chemically random Ta-W alloys, electronic structure calculations were carried out on the basis of the charge self-consistent fully relativistic version of the TB-LMTO-CPA method within the atomic sphere approximation (ASA) and the local-density approximation (LDA) of density-functional theory. The LDA calculations were based on the exchange-correlation energy of Ceperley and Alder[10] as parametrized by Perdew and Zunger.[11] To eliminate the charge-transfer effects, at each lattice parameter and alloy composition, the atomic sphere radii of the two species were adjusted in such a way that atoms were charge neutral while preserving the total volume of the alloy. In our calculations we used 168 **k** points in the irreducible wedge of the Brillouin zone to perform the integrations that are necessary during the self-consistent calculations, and 2320 **k** points in the full Brillouin zone for the calculation of the ECI. We use 12 energy points on a semicircle in the upper half-plane of complex energy to perform the energy integration using Gauss' method. The densities of states were evaluated on a line 0.005 Ry above the real axis (with an energy step of about 5 mRy) and then deconvoluted on the real axis. The CPA equations were solved iteratively using the method described in Ref. 8.

In Fig. 1 we display the density of states (DOS) of chemically random Ta-W alloys at various compositions. Note that when going from pure W for which the number of valence electrons $N_v=5$ to pure Ta with $N_v=4$, the Fermi energy spans a deep minimum of density of states that clearly separates the bonding and antibonding states in the alloy band structure. This minimum in the DOS is, to some extent, related to a negative energy of formation, more so for the tungsten-rich alloys. Since the two alloy species are neighbors in the periodic table, the scattering properties of the electrons and therefore the DOS's remain practically unchanged with alloy composition. Thus the variation of the electronic structure properties with alloy composition is almost entirely reflected in the variation of N_v, and therefore the location of the Fermi energy as would be the case for an alloy treated within the virtual crystal approximation.

In Fig. 2(a), we show the variation of the equilibrium lattice parameter, a^{eq} of the chemically random Ta-W alloy with composition together with the experimentally assessed lattice parameter-composition relation represented by $a=3.164+0.1054\ c_{Ta}+0.03226\ c_{Ta}^2$ in Å.[2] As usual, there is about a 1% discrepancy between the theoretical and experimental values of lattice constant, but as seen in Fig. 2(b), the departure from Vegard's law, given by $\delta a^{eq}=a^{eq}_{alloy}-c_{Ta}a^{eq}_{Ta}-(1-c_{Ta})a^{eq}_{W}$ (where a_i^{eq} is the equilibrium lattice constant of the pure element i) is accurately reproduced by this electronic structure method. This result strongly suggests that alloy formation is favored and leads to a more compact structure than a simple combination of both alloy species would.

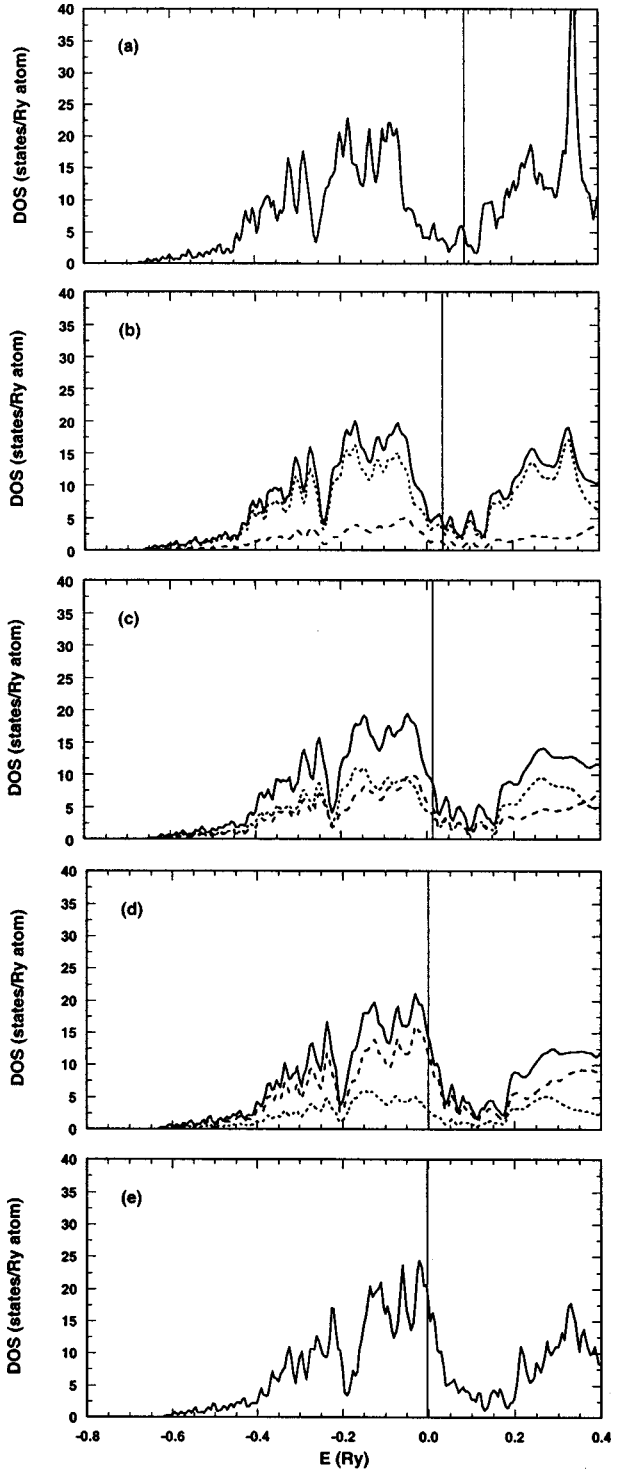

FIG. 1. Density of states of bcc-based Ta-W disordered alloys as a function of energy (the Fermi energy E_F is indicated by a vertical line) and of Ta concentration $c_{Ta}=0,1/4,1/2,3/4,1$ (from top to bottom), as obtained from TB-LMTO-CPA. In the alloy case, the solid line indicates the total density of states, whereas the dotted (dashed) line refers to the partial densities of states of Ta (W).

Figure 3 displays the variation of the bulk modulus with composition. For the pure elements, there is a typical 15% discrepancy between predicted and measured values. One should note that, as observed experimentally, a one-valence

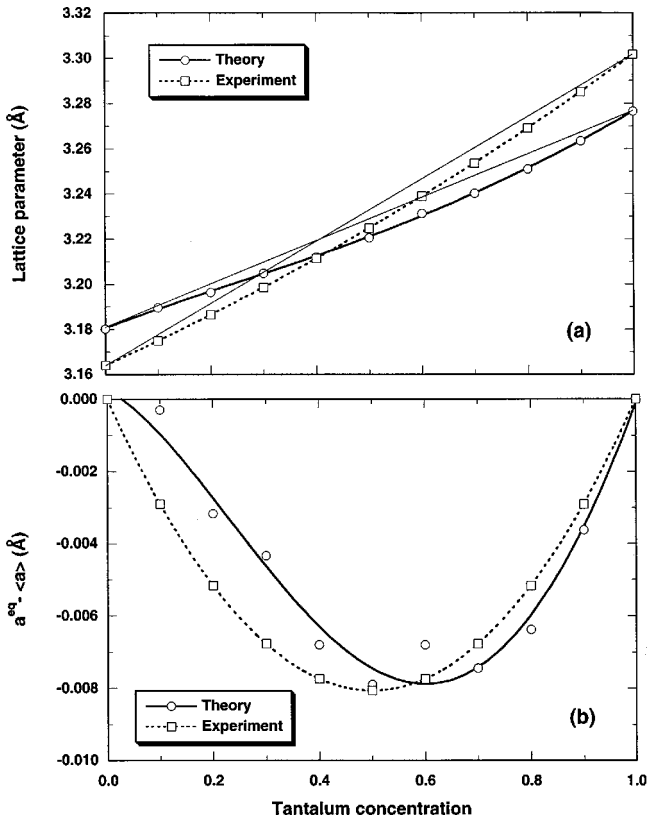

FIG. 2. Variation of (a) the bcc lattice constant a^{eq} (in Å) of the chemically random alloy Ta-W and (b) of the departure from Vegard's law, δa^{eq} (in Å) with Ta concentration. The solid line corresponds to the theoretical results and the dotted line to the experimental data from Ref. 2.

electron variation leads to a decrease by almost a factor 2 in the bulk modulus when going from W to Ta.

For comparison purposes, we report in Table I the equilibrium lattice constant and bulk modulus for the pure species, obtained by three *ab initio* approaches. Method 1 refers to the standard scalar relativistic LMTO-ASA (Ref. 12) with inclusion of so-called combined corrections that account for overlap of atomic spheres and for higher partial waves inside the atomic spheres, and with exchange and correlation potential proposed by von Barth and Hedin.[13] Method 2 corresponds to the full-potential LMTO (FP-LMTO) (Refs. 14 and 15) that includes nonspherical terms within the muffin-tin spheres and provides a fully relativistic (semirelativistic) treatment of the core (valence) electrons, with spin-orbit coupling taken into account for the valence electrons. The exchange and correlation potential has the form proposed by Ceperley and Adler[10] and parametrized by Perdew and Zunger.[11] Finally, method 3 corresponds to the fully relativistic TB-LMTO-ASA-CPA, that has been selected in this work for its applicability to off-stoichiometric alloys (including the pure elements), whereas the other two are only applicable to stoichiometric alloys (and pure elements) describable by supercells. Note that all three methods give values for the lattice constant and the bulk modulus, which are within the error expected from any LDA calculation.

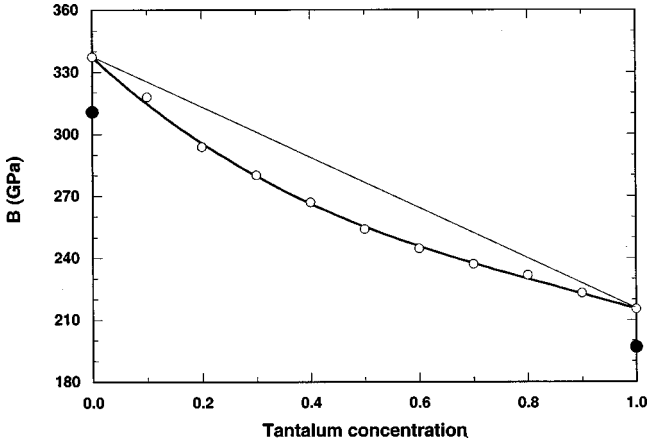

FIG. 3. Variation of the bulk modulus (in GPa) of the bcc-based chemically random Ta-W alloy with Ta concentration. The solid circles indicate the experimental value of the endpoints.

Finally in Fig. 4 we show the variation of the formation (or mixing) energy of the chemically random alloy with composition. This energy is given by

$$\Delta E_{\mathrm{mix}} = E^{\mathrm{CPA}}_{\mathrm{alloy}} - c_{\mathrm{Ta}} E^{\mathrm{eq}}_{\mathrm{Ta}} - (1 - c_{\mathrm{Ta}}) E^{\mathrm{eq}}_{\mathrm{W}}, \qquad (2.1)$$

where $E^{\mathrm{CPA}}_{\mathrm{alloy}}$ is the total energy of the alloy described within the CPA at its equilibrium lattice parameter, and E^{eq}_{i} is the total energy of pure species i at its corresponding equilibrium lattice parameter. This mixing energy is negative in the case of Ta-W with a maximum value of -9.36 mRy/atom at a tantalum concentration of about 0.375. Hence, the energetics favors the formation of the disordered alloy configuration in the whole range of alloy composition. This result confirms a previous conclusion drawn from a semiempirical tight-binding estimation of the energy of formation of the random Ta-W alloy as a function of composition.[16] However in this study, the tight-binding energies are underestimated by about 40%, and the general evolution of the formation energy with alloy composition does not reveal any asymmetry as it should since the DOS at the Fermi energy that controls the strength of the bonding in this alloy varies significantly with the number of valence electrons.

III. GROUND-STATE PROPERTIES

In recent years a number of methods have been developed[9] to map the quantum-mechanical description of the energetics of an alloy in the form of an Ising model that is most appropriate for a subsequent statistical mechanics treatment of order-disorder phenomena in alloys as functions of temperature and concentration. This mapping has been originally achieved within the so-called GPM (Refs. 4 and 5) which is the method that will be used here. Within the GPM, only the configuration-dependent contribution to the total energy is expressed by an expansion in terms of effective pair and multisite interactions, and since the reference medium is concentration dependent, so are these interactions. One should emphasize that this method is in contrast with the one based on the knowledge of the electronic structure properties of ordered configurations of the alloy, such as the so-called Connolly-Williams method,[17] which leads to an expansion of

TABLE I. Equilibrium properties, i.e., lattice constant (in Å), bulk modulus (in GPa), and when applicable the formation energy of the ordered $B2$ phase (in mRy/atom), of bcc-based pure Ta and W, and of the $B2$ ordered phase of TaW. Methods 1 to 3 correspond to LMTO-ASA, FP-LMTO,[15] and TB-LMTO-ASA in the case of the pure species or TB-LMTO-CPA-GPM in the case of the ordered $B2$ phase of TaW, respectively.

Property	Method	Pure Ta	Pure W	Ordered $B2$ TaW
Lattice constant	Experiment	3.3031	3.1652	N/A
(in Å)	Method 1	3.3098	3.1934	3.2421
	Method 2	3.2518	3.1438	3.1890
	Method 3	3.2766	3.1802	3.2203
Bulk modulus	Experiment	196.1	310.4	N/A
(in GPa)	Method 1	206.4	314.0	255.8
	Method 2	208.8	333.1	269.2
	Method 3	215.3	337.3	276.8
$\Delta E_{\text{form}}^{\text{B2}}$	Method 1	N/A	N/A	−8.0
(in mRy/atom)	Method 2	N/A	N/A	−8.5
	Method 3	N/A	N/A	−13.0

the total energy itself in terms of cluster interactions that are concentration independent, except via volume effects. Within the GPM, the ordering contribution to the total energy of an A-B alloy is given by

$$\Delta E_{\text{ord}}(\{p_n\}) = \sum_{k=1}^{\infty} \frac{1}{k} {\sum_{n_1,\ldots,n_k}}' V^{(k)}_{n_1\ldots n_k} \delta c_{n_1} \cdots \delta c_{n_k}, \tag{3.1}$$

where δc_{n_i} refers to the fluctuation of concentration on site n_i, $\delta c_{n_i} = p_{n_i} - c$, where c is the concentration in B species, and p_{n_i} is an occupation number associated with site n_i, equal to 1 or 0 depending on whether or not site n_i is occupied by a B species. The $V^{(k)}_{n_1\ldots n_k}$ corresponds to a kth-order ECI involving a cluster of k sites. The prime in the summation over the $\{n_i\}$ indicates that consecutive site indices must be different. Note that, as in any perturbation theory that relies on the CPA medium, the small parameter in the GPM only depends on the scattering properties of the electrons, which means that the expansion for the ordering energy is valid even for large fluctuations of local concentration. In practice, the second-order contribution to the ECI, $V^{(2)}_{nm}$ is, within the GPM, essentially numerically indistinguishable from the full summation of all scattering processes taking place between the two sites n and m. Hence, to second order in perturbation and for alloys based on simple lattices described by one type of site per cell, such as bcc, Eq. (3.1) is rewritten as

$$\Delta E_{\text{ord}}(\{p_n\}) \simeq \sum_s V^{(2)}_{0s} \delta c_0 \delta c_s \tag{3.2}$$

or equivalently, at zero temperature

$$\Delta E_{\text{ord}}(\{q_s\}) \simeq \sum_s q_s V_s \tag{3.3}$$

with $q_s = \frac{c}{2}(n_s^{\text{BB}} - c n_s)$, where n_s^{BB} and n_s refer to the number of BB pairs and the total number of pairs per site, respectively, associated with the sth-neighbor shell, and c is the concentration in B species. In this last equation, V_s represents a sth-neigbor effective pair interaction (EPI) given by $V_s = V_s^{\text{AA}} + V_s^{\text{BB}} - 2V_s^{\text{AB}}$, and by definition corresponds to the second-order interaction between a site at the origin and a site belonging to the sth-neighbor shell $V^{(2)}_{0s}$ entering Eq. (3.2). Hence, the sign convention that has been adopted is such that when $V_s > 0$ (<0), AB (AA or BB) pairs associated with a species at the origin and the other in the sth-neighbor shell are favored.

As seen from Eq. (3.3), any alloy configuration is specified by a unique set of parameters $\{q_s\}$ that only depends on site occupancies. For example, at zero temperature and for $s = 1$–5, these parameters take the values -1, 3/4, 3/2, -3,

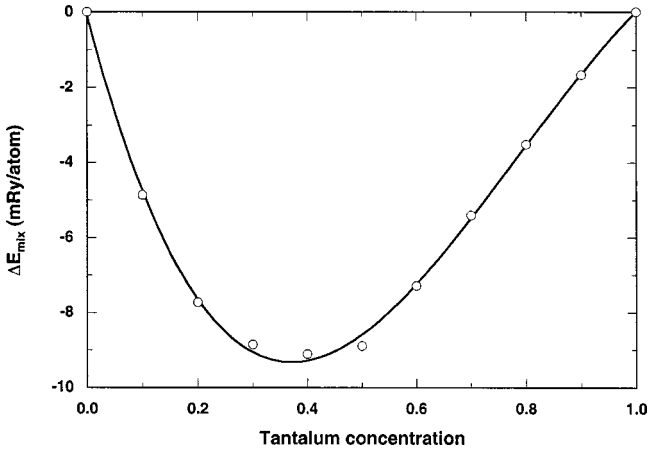

FIG. 4. Variation of the mixing energy ΔE_{mix} (in mRy/atom) of the bcc-based chemically random Ta-W alloy with Ta concentration.

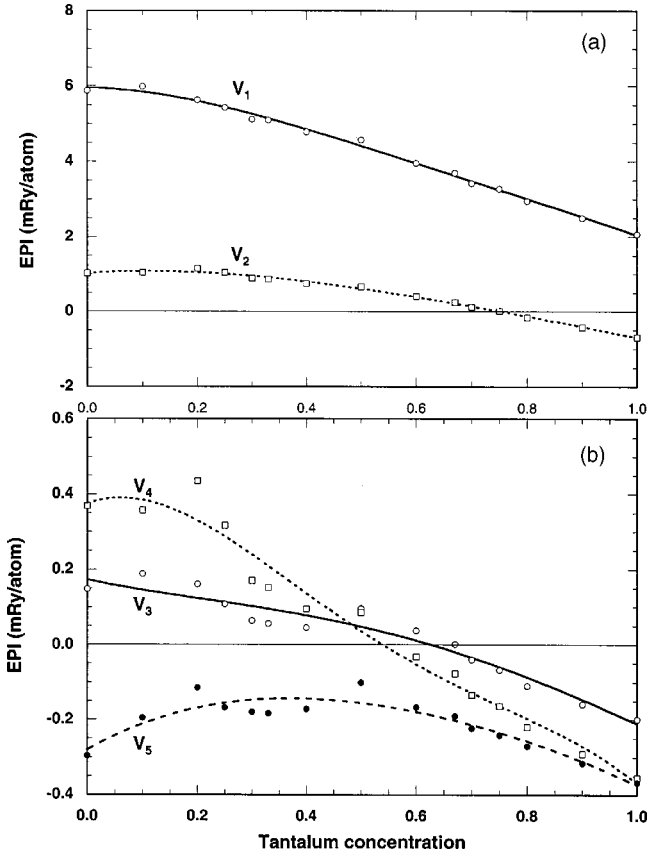

FIG. 5. Effective pair interactions $V_s^{(2)}$ (where s is the shell index), in mRy/atom, as functions of Ta concentration for bcc-based Ta-W alloys, as obtained from TB-LMTO-CPA-GPM: (a) for $s=1,2$ and (b) for $s=3-5$.

1 for $B2$ order (of CsCl type) at equiatomic composition and $-1/4$, $-3/16$, $9/8$, $-3/4$, $-1/4$ for $D0_3$ order (of Fe_3Al type) at $c=1/4,3/4$. In the case of the Ta-W alloy system, the EPI's were computed from the knowledge of the electronic structure of the chemically random alloy at each composition and lattice parameter.[5,8,9] In Fig. 5 the EPI's up to the fifth neighbor shell are plotted as functions of alloy composition at the equilibrium lattice parameter and Fermi energy of the corresponding chemically random alloy. As expected, the first two EPI's are an order of magnitude larger than the more distant interactions, with a ratio $V_1/V_2 \geqslant 0$ for $c_{\mathrm{Ta}} \leqslant 0.76$. In Fig. 6, we show that the EPI's, here given for the stoichiometric $Ta_{50}W_{50}$ alloy converge rapidly with distance, a property that is valid in the whole range of composition. Also, we found that the EPI's vary very little as a function of lattice parameter (not shown), and therefore with pressure, at any alloy composition.

From the results of the ground-state analysis of the Ising model, the most probable ground states at zero temperature can be predicted. The most extensive study of the Ising Hamiltonian applied to the bcc lattice includes up to the fifth neighbor pair interaction (with the exclusion of V_4) in the analysis.[5,18–20] With the EPI's displayed in Fig. 5, and if one only considers V_1 and V_2 in the expansion given by Eq. (3.3) and in the analysis,[21] it is concluded that, at zero temperature, there exist two ground states: the $D0_3$ ordered phase for

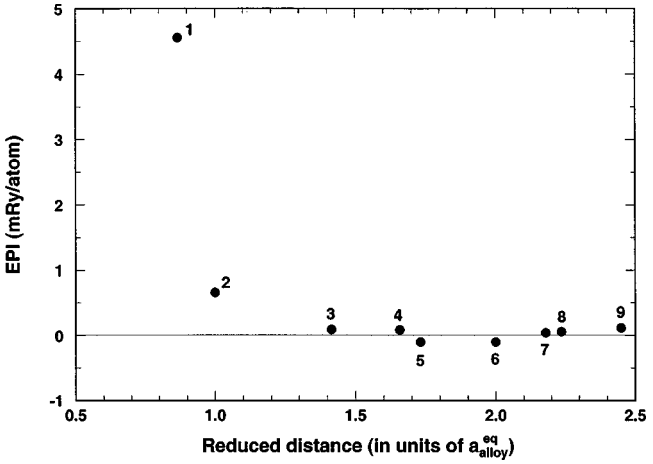

FIG. 6. Effective pair interactions $V_s^{(2)}$, or EPI's (in mRy/atom) as functions of the reduced distance d/a^{eq} for $Ta_{50}W_{50}$, where a^{eq} corresponds to equilibrium lattice parameter of the alloy, as obtained from TB-LMTO-CPA-GPM.

TaW_3, and to a less extent Ta_3W, and the $B2$ ordered phase for TaW, with the corresponding ordering energies equal to about -1.55, $-.82$, and -4.07 mRy/atom, respectively. Since the EPI's beyond second-nearest neighbors are small, see Fig. 6, the results of the analysis remain the same, with minor modification in the magnitude of the ordering energies quoted above. Overall, the ordering tendencies are stronger for the W-rich Ta-W alloys, and this trend is consistent with what is expected for transition metal alloys.[5,9] Indeed, the variation of the dominant EPI's with the number of d electrons displays in general two zeros that are located around three and seven d electrons, with a positive sign of the EPI's in the central region. Although the location of the zeros varies with the scattering properties of the electrons and alloy composition, heteroatomic pairs are increasingly favored when the number of d electrons increases from Ta (about 3.3) to W (about 4.4) in the Ta-W case, which is what Fig. 5 shows in a more quantitative way.

To confirm the GPM predictions, calculations were performed with methods 1 and 2 described in Sec. II, and compared with those of method 3, i.e., TB-LMTO-CPA-GPM within the ASA, to study the equilibrium properties and the energetics of the ordered $B2$ phase of $Ta_{50}W_{50}$. In the case of method 3, the energy of formation of the ordered configuration $B2$ is given by $\Delta E_{\mathrm{form}}^{\mathrm{B2}} = \Delta E_{\mathrm{mix}} + \Delta E_{\mathrm{ord}}^{\mathrm{B2}}$, see Eqs. (2.1) and (3.3). The equilibrium lattice constant of the $B2$ phase was obtained by minimizing the energy $\Delta E_{\mathrm{form}}^{\mathrm{B2}}$ with respect to volume since, from the CPA and the GPM calculations, the variation with volume of ΔE_{mix} and of the EPI's that built up the ordering energy $\Delta E_{\mathrm{ord}}^{\mathrm{B2}}$ are known. The results of all three methods, reported in Table I, are consistent in the sense that the formation energy of the ordered $B2$ phase, of the order of -10 mRy/atom, is negative and therefore favors phase formation. The variation in the results, within the error expected from any LDA calculation, reflects the various levels of approximation that characterize each method: ASA versus no-shape approximation, form of exchange-correlation potential, and scalar relativistic versus fully rela-

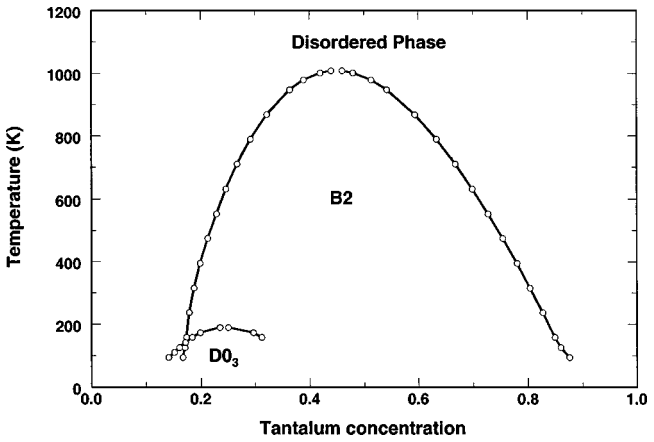

FIG. 7. Predicted bcc-based Ta-W phase diagram, as obtained from the tetrahedron approximation of the CVM.

tivistic treatment. However, one can note that the departure of the lattice constant from Vegard's law given by all three methods is about -0.008 Å, once again consistent with a tendency towards alloy formation and order.

IV. STABILITY AT FINITE TEMPERATURE

By making use of the energetics presented in Secs. II and III the Ising model has been solved within a generalized mean-field approximation with the CVM. At each temperature and alloy composition, the configurational part of the free energy has been minimized with a Newton-Raphson technique with respect to the correlation functions defined as the following thermodynamical average product

$$\xi_\alpha = \langle \sigma_1 \cdots \sigma_\alpha \rangle, \tag{4.1}$$

where σ_n correspond to the so-called spin variable related to the occupation number p_n by $\sigma_n = 2p_n - 1$, and the maximum value of α correspond to the number of sites in the maximum cluster that characterizes the level of approximation of the CVM. In the present case, the maximum cluster corresponds to the irregular tetrahedron made of four first and two second-nearest-neighbor pairs.[22] This cluster allows a proper statistical treatment with the EPI's V_1 and V_2 included in the pair expansion of the Ising model, an approximation that is justified here since the more distant EPI's have negligible amplitude, see Figs. 5 and 6. The predicted phase diagram is presented in Fig. 7. Considering the high melting point of the alloy species, the $B2$ and $D0_3$ ordered phases of Ta-W alloys are stable at low temperature, not exceeding a 1000 K. Note that around the stoichiometry Ta_3W, we ignored the region of stability of the $D0_3$ ordered structure that, according to its energetics, should exist at temperatures below 100 K. The asymmetry of the phase diagram is a direct consequence of the energetics of Ta-W alloys, i.e., an extremum of energy of mixing, see Fig. 4, and stronger ordering trends, see Fig. 5, for W-rich alloys. Since below $c_{\mathrm{Ta}} \leqslant 0.76$ the ratio $V_2/V_1 < 2/3$, the phase diagram exhibits typical features.[5,22] In particular, the transition from the disordered to the $D0_3$ state is first order, whereas the one between the $B2$ and the $D0_3$ ordered states is almost everywhere second order in accordance with the results of the Landau theory of phase transitions.

Since the elastic properties of Ta and W are quite different, the vibrational free energy was estimated to study its impact on the alloy free energy and thus on the phase diagram. To this end, we followed the procedure proposed in Ref. 23. The vibrational contribution to the free energy is expressed within the well-known Debye approximation. The Debye temperature for the alloy is written as

$$\Theta_{\mathrm{D}} \simeq \langle K \rangle (r_{\mathrm{WS}} B_m / \langle M \rangle)^{1/2}, \tag{4.2}$$

where $\langle X \rangle$ refers to a concentration weighted average of the quantity X associated with the pure species, r_{WS} is the Wigner-Seitz radius which, in the case of a bcc lattice, is related to the lattice constant a by $r_{\mathrm{WS}} = (3/8\pi)^{1/3} a$, B_m is the bulk modulus evaluated at r_{WS}, M is the atomic mass, and K is a constant of proportionality. From the relation between Debye temperature and bulk modulus for the pure species, and with $\Theta_{\mathrm{D}}^{\mathrm{Ta}} \simeq 240$ K and $\Theta_{\mathrm{D}}^{\mathrm{W}} \simeq 400$ K, then $K_{\mathrm{Ta}} \simeq 39.844$ and $K_{\mathrm{W}} \simeq 54.289$. Despite the noticeable difference in the elastic properties of Ta and W, the vibrational free energy is more than an order of magnitude smaller than the CVM free energy. For example, at $T = 1200$ K, at equiatomic composition, the vibrational free energy is about -0.27 mRy/atom, compared with the configurational free energy of the order of -14.19 mRy/atom. Hence the vibrational free energy has little effect on the predicted phase diagram displayed in Fig. 7.

To compare the experimental thermodynamic assessment of Ta-W alloys[3] to our predicted data, the individual activities a_i ($i = \mathrm{Ta}, \mathrm{W}$) have been determined as a function of tantalum concentration at $T = 1200$ K. These quantities are related to the excess grand potential $\delta\Omega$ as follows[24]

$$a_{\mathrm{Ta}} = \exp[(\delta\Omega + \mu)/k_{\mathrm{B}}T],$$

$$a_{\mathrm{W}} = \exp[(\delta\Omega - \mu)/k_{\mathrm{B}}T], \tag{4.3}$$

where k_{B} is the Boltzmann's constant, and μ is the chemical potential difference $\mu = (\mu_{\mathrm{Ta}} - \mu_{\mathrm{W}})/2$. As usual, the grand potential is given by $\delta\Omega = \delta F - \mu(2c_{\mathrm{Ta}} - 1)$, with δF being the configurational free energy. The results of the comparison are displayed in Fig. 8. Although the negative departure from linearity is confirmed by the calculations, the discrepancies between prediction and experimental assessment may be attributed to the low temperature of 1200 K at which the experiments were carried out where equilibrium is difficult to reach, a remark that is certainly applicable to this refractory alloy system. However, from both our study and the experimental results,[3] the negative departure of the elemental activities from Raoult's law, i.e., from ideality, clearly indicates a tendency towards not only formation of the Ta-W solid solution but also chemical SRO.

Although a low-lying phase diagram is predicted in the solid phase, one can expect the SRO to remain quite strong at high temperature, well above the critical order-disorder line since the $B2$ to disorder transition is second order in nature. To show that property, we calculated a quantity proportional to the intensity of diffuse scattering, $I_{\mathrm{SRO}}(\mathbf{k})$, de-

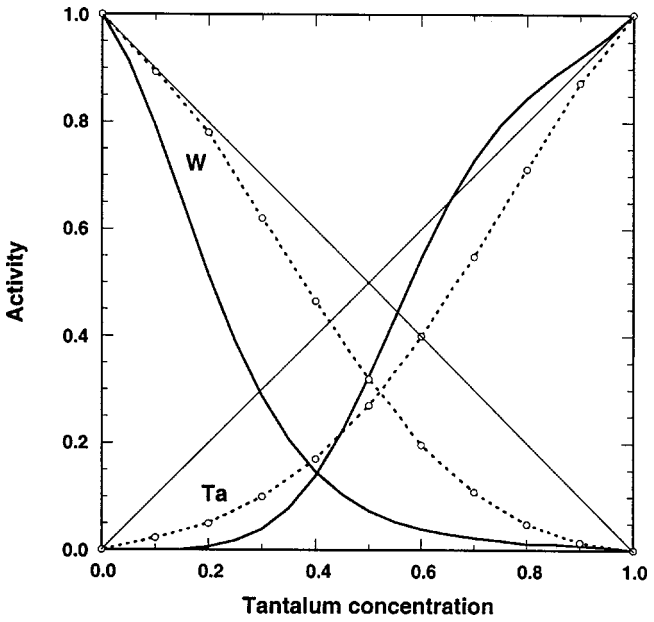

FIG. 8. Activities of tantalum and tungsten in the Ta-W alloy system at 1200 K: calculated (solid line) and experimentally assessed (dotted line) from Ref. 3.

scribed in **k** space and given within the Krivoglaz-Clapp-Moss (KCM) approach[25,26] by

$$I_{\mathrm{SRO}}(\mathbf{k}) \simeq \frac{1}{1+c(1-c)\beta V(\mathbf{k})}, \tag{4.4}$$

where $\beta = 1/k_{\mathrm{B}}T$ and $V(\mathbf{k})$ is the Fourier transform of the EPI's. As expected, a minimum in $V(\mathbf{k})$ for some special **k** point leads to a maximum of intensity of diffuse scattering, with a divergence of the intensity at the critical order-disorder temperature T_{c} according to the results of the single-site mean-field theory on which the KCM approach is based. In Fig. 9(a) the SRO diffuse-scattering intensity is displayed in the (001) plane in the reciprocal space for Ta-W at equiatomic composition at $T = 2000$ K. The maxima of intensity show up at the $2\pi/a(100)$ (where a is the lattice constant) and equivalent positions, which correspond to the superlattice reflections of the $B2$ ordered phase. Note that even well above the critical order-disorder line the intensity remains strong as was anticipated, and that the SRO persists far away from the equiatomic composition as shown in Fig. 9(b) for a $Ta_{90}W_{10}$ alloy at $T = 1500$ K.

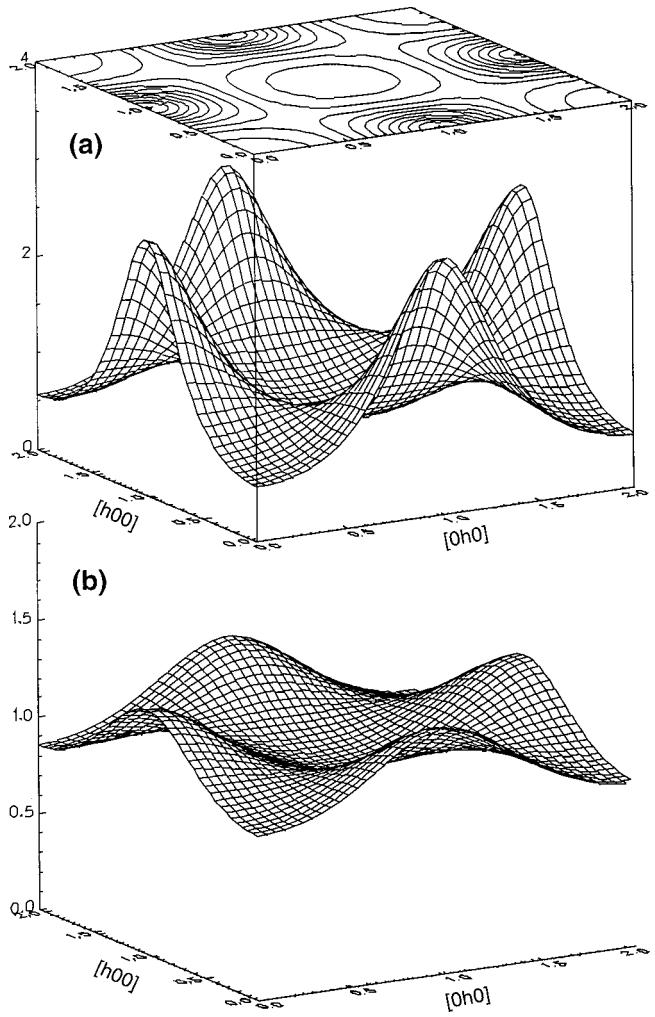

FIG. 9. Short-range order diffuse intensity in the (001) plane for bcc-based $Ta_{50}W_{50}$ at $T = 2000$ K (a), and $Ta_{90}W_{10}$ at $T = 1500$ K (b).

V. CONCLUSION

We have carried out detailed calculations on electronic structure and related thermodynamic properties of Ta-W alloys using the TB-LMTO formulation of the coherent potential approximation. We have also compared some of our results with those obtained through different methodologies. The CPA and the GPM were used to obtain ordering tendencies and related thermodynamic information across the concentration range of these alloys. Temperature effects were accounted for within the generalized mean-field approach on which the CVM is based.

Our main conclusion, and a prediction that results from this work, is that Ta-W alloys exhibit a strong tendency towards order with a $B2$ superstructure in a broad range of alloy composition. This should not come as a surprise since experimentally there were indications that this alloy system should not follow an ideal law of mixing. This result is consistent with the behavior of quantities related to the ordering tendencies of alloys, such as the negative departure from Vegard's law of the equilibrium lattice constant and the negative departure from Raoult's law of the activity of each species, as a function of alloy concentration. This departure was found in all of our calculations, those of disordered alloys based on the CPA and those of the electronic structure of stoichiometric compounds obtained using different methodologies. Similar general agreement among the results of different electronic structure methods was found with respect to other quantities of interest, such as the bulk modulus.

Although the solid-phase part of the phase diagram is predicted at low temperature, relatively to the location of the solidus-liquidus line, the second-order nature of the transition from $B2$ to the disordered state can be used advantageously to identify the short-range order in this alloy, at tem-

peratures as high as 2500 K. Anomalous dispersion x-ray diffuse-scattering measurements at a synchrotron source[27] or neutron-diffraction experiments should reveal unambiguously the nature of the short-range order on samples well annealed at relatively high temperature to promote the thermally activated ordering process. This work will be extended to all combinations of refractory metals of columns VB and VIB of the periodic table to understand how electronic structure properties affect stability and order in this class of alloys. This is particularly relevant since the 15 possible assessed phase diagrams made of these metals and their alloys show either miscibility gap or complete miscibility in the solid phase. Series effect ($3d$ vs $4d$ vs $5d$: intra- or inter-series alloy combination) and variation in the difference of the numbers of valence electrons (0 or 1) are expected to dictate the ordering trends in a rational way, and this will be presented in a forthcoming paper.

ACKNOWLEDGMENTS

This work was performed under the auspices of the U.S. Department of Energy by the Lawrence Livermore National Laboratory under Contract No. W-7405-ENG-48. Financial support from the Grant Agency of the Academy of Sciences of the Czech Republic, Project No. 1010829, and the U.S.-Czechoslovak Science and Technology Program, Project No. 95-018, is gratefully acknowledged.

[1] *Binary Alloy Phase Diagrams*, edited by T. B. Massalski (ASM International, Materials Park, OH, 1990), Vols. 1–3.
[2] R. Krishnan, S.P. Garg, and N. Krishnamurthy, J. Alloy Phase Diagrams **3**, 1 (1987).
[3] S.C. Singhal and W.L. Worrell, Metall. Trans. **4**, 895 (1973).
[4] F. Ducastelle and F. Gautier, J. Phys. F: Met. Phys. **6**, 2039 (1976).
[5] F. Ducastelle, in *Order and Phase Stability in Alloys*, edited by F. R. de Boer and D. G. Pettifor, Cohesion and Structure series, vol. 3. (North-Holland, Amsterdam, 1991).
[6] J. S. Faulkner, in *Progress in Materials Science*, edited by J. W. Christian, P. Hassen, and T. B. Massalski (Pergamon Press, New York, 1982), Vol. 27, No. 1 and 2, and references cited therein.
[7] R. Kikuchi, Phys. Rev. **81**, 988 (1951).
[8] I. Turek, V. Drchal, J. Kudrnovský, M. Šob, and P. Weinberger, *Electronic Structure of Disordered Alloys, Surfaces and Interfaces* (Kluwer, Boston, 1997).
[9] P. E. A. Turchi, in *Intermetallic Compounds: Principles and Practice*, edited by by J. H. Westbrook and R. L. Fleischer (Wiley, New York, 1995), Vol. 1, Chap. 2, pp. 21–54.
[10] D.M. Ceperley and B.J. Alder, Phys. Rev. Lett. **45**, 566 (1980).
[11] J.P. Perdew and A. Zunger, Phys. Rev. B **23**, 5048 (1981).
[12] H. L. Skriver, *The LMTO Method*, Springer Series in Solid-State Sciences Vol. 41 (Springer-Verlag, Heidelberg, 1983); O. K. Andersen, O. Jepsen, and D. Glötzel, in *Highlights of Condensed Matter Theory*, edited by F. Bassani, F. Fumi, and M. P. Tosi (North-Holland, Amsterdam, 1985), p. 59.
[13] U. von Barth and L. Hedin, J. Phys.: Condens. Matter **5**, 1629 (1972).
[14] D.L. Price and B.R. Cooper, Phys. Rev. B **39**, 4945 (1989).
[15] N. Kioussis (private communication).
[16] C. Colinet, A. Bessoud, and A. Pasturel, J. Phys. F: Met. Phys. **18**, 903 (1988).
[17] J.W.D. Connolly and A.R. Williams, Phys. Rev. B **27**, 5169 (1983).
[18] A. Finel and F. Ducastelle, in *Phase Transformations in Solids*, edited by T. Tsakalakos (North-Holland, Amsterdam, 1984), p. 293.
[19] A. Finel, D. Gratias, and R. Portier, in *L'Ordre et le Désordre dans les Matériaux* (Les Editions de Physique, Les Ulis, 1984), p. 9.
[20] A. Finel, Thèse de Doctorat d'Etat es Sciences Physiques, University Paris VI, France, unpublished (1987); and Technical Report No. ONERA 1987-3 (unpublished).
[21] S.M. Allen and J.W. Cahn, Acta Metall. **20**, 423 (1972).
[22] N.S. Golosov and A.M. Tolstik, J. Phys. Chem. Solids **36**, 899 (1975).
[23] V.L. Moruzzi, J.F. Janak, and K. Schwarz, Phys. Rev. B **37**, 790 (1988).
[24] C. Bichara and G. Inden, in *Statics and Dynamics of Alloy Phase Transformations*, Vol. 319 of *NATO Advanced Studies Institute, Series B: Physics*, edited by P. E. A. Turchi and A. Gonis (Plenum Press, New York, 1994), p. 541.
[25] M. A. Krivoglaz, *Theory of X-Ray and Thermal Neutron Scattering by Real Crystals* (Plenum Press, New York, 1969).
[26] P.C. Clapp and S.C. Moss, Phys. Rev. **171**, 754 (1968).
[27] G.E. Ice, C.J. Sparks, A. Habenschuss, and L.B. Shaffer, Phys. Rev. Lett. **68**, 863 (1992); L. Reinhard, J.L. Robertson, S.C. Moss, G.E. Ice, P. Zschack, and C.J. Sparks, Phys. Rev. B **45**, 2662 (1992).